DOI:10.16555/j.1006-8775.2014.02.006

Article ID: 1006-8775(2014) 02-0143-11

THE DOWNSCALING FORECASTING OF SEASONAL PRECIPITATION IN GUANGDONG BASED ON CLIMATE FORECAST SYSTEMS PRODUCTS

LI Chun-hui (李春晖)[1], LIN Ai-lan (林爱兰)[1], GU De-jun (谷德军)[1], WANG Ting (王　婷)[2], PAN Wei-juan (潘蔚娟)[2], ZHEN Bin (郑　彬)[1]

(1. Guangzhou Institute of Tropical and Marine Meteorology/Guangdong Provincial Key Laboratory of Regional Numerical Weather Prediction, China Meteorological Administration, Guangzhou 510080 China; 2. Guangdong Climate and Agrometeorological Center, Guangzhou 510080 China)

Abstract: The Climate Forecast Systems (CFS) datasets provided by National Centers for Environmental Prediction (NCEP), which cover the time from 1981 to 2008, can be used to forecast atmospheric circulation nine months ahead. Compared with the NCEP datasets, CFS datasets successfully simulate many major features of the Asian monsoon circulation systems and exhibit reasonably high skill in simulating and predicting ENSO events. Based on the CFS forecasting results, a downscaling method of Optimal Subset Regression (OSR) and mean generational function model of multiple variables are used to forecast seasonal precipitation in Guangdong. After statistical analysis tests, sea level pressure, wind and geopotential height field are made predictors. Although the results are unstable in some individual seasons, both the OSR and multivariate mean generational function model can provide good forecasting as operational tests score more than sixty points. CFS datasets are available and updated in real time, as compared with the NCEP dataset. The downscaling forecast method based on the CFS datasets can predict three seasons of seasonal precipitation in Guangdong, enriching traditional statistical methods. However, its forecasting stability needs to be improved.

Key words: CFS; Optimal Subset Regression; mean generational function; Guangdong; precipitation; downscaling

CLC number: P456.8 **Document code:** A

1 INTRODUCTION

Located in a monsoon zone of low-latitude East Asia, Guangdong province is subject to complicated weather and climate systems and both the subtropical and tropical monsoons pose tremendous influence on it. Consequently, abnormal precipitation occurs frequently during the flood season, causing huge economic losses. Being of great importance to disaster prevention and mitigation, the research on the precipitation of Guangdong aims at improving the prediction of long-term tendencies of precipitation and eventually setting up a new system of operational forecast. The air-ocean global climate model (AOGCM) is currently the most important and feasible method for estimating large-scale future climate across the globe, but it is not suitable for making accurate prediction of regional climate as it has low spatial resolution and lacks information on regional climate. Currently, two methods are able to make up for the insufficiency of AOGCM in this aspect, one being higher versions of AOGCM and the other the downscaling method. As huge computation is needed to improve the current AOGCM, downscaling becomes a primary approach. It is developed based on the argument that the scenario of regional climate is made on the conditions of large-scale (e.g. continental or even planetary scale) climate[1, 2] and as a result, the restrains of AOGCM

Received 2013-04-25; **Revised** 2014-01-29; **Accepted** 2014-04-15

Foundation item: Science and Technology Program for Guangdong Province (2005B32601007); Project of Guangdong Meteorological Bureau (2008B05); Natural Science Foundation of China "Project 973" (2010CB950304); Project of Meteorological Science and Technology of Guangdong Province (200902); Project for Science and Technology Planning in Guangdong (2012A061400012); Science Project for Guangdong Meteorological Bureau (2013B08); Project for Guangdong Provincial Bureau of Science and Technology (2012A030200006); Project for Meteorological Center of the South China Region, China Meteorological Administration (GRMC2012M02); Science and Technology Planning Project for Guangdong Province (2011A032100006, 2012A061400012)

Biography: LI Chun-hui, associate professor, M.S., primarily undertaking research on monsoon and tropical weather and climate.

Corresponding author: LI Chun-hui, e-mail: chli@grmc.gov.cn

can be overcome by transforming the output of the large-scale and low-resolution AOGCM into information about surface climate change (like air temperature and precipitation) on the regional scale. At present, there are two ways of downscaling, either dynamically or statistically. Relatively speaking, the latter involves smaller amount of computation and shorter hours of computer runs, applicable for many different types of AOGCM.

Although the statistical downscaling method has been extensively applied in estimation of future regional climate change outside China, it is rarely seen inside it. Lu et al.[3] worked on how to process initial data in downscaling and Chen et al.[4] investigated the use of downscaling in monthly precipitation forecast with the summary that it has achieved good results in forecasting the precipitation in China through the technique of ensemble forecast using T63/NCC monthly dynamic extended situation fields. With a downscaling model that combines primary component analysis with stepwise regression, Fan et al.[5] estimated the scenario of climate change in North China under different HadCM3 assumptions. As also shown in their real-case study of regional climate scenario of river basins, Ding et al.[6] estimated regional daily maximum, minimum temperature and precipitation in the 50 years ahead and predicted good climate extremes using statistical downscaling that combines primary component analysis with optimal subset regression (hereafter OSR). With an established downscaling forecasting method for monthly precipitation in Guangxi based on a BP neural network model, He et al.[7] pointed out that both the fitting accuracy and forecasting capabilities of models with current factors are better than those with preceding ones. Using the data of monthly 500-hPa geopotential heights of the Northern Hemisphere from 1951 to 2007 and the methods of downscaling and partial least squares regression, Wei et al.[8] studied the predictability of June–August precipitation in eastern China and concluded that the 500-hPa geopotential heights from 40°E to 180° in East Asia are a relatively good field of downscaling factors.

In this paper, the products from Climate Forecast Systems (CFS), a climate forecasting system developed at the National Centers for Environmental Prediction (NCEP, USA), are used. Since its operational run from August 2004, CFS has become an important tool for the monthly and seasonal forecast of climate at NCEP. CFS is a dynamic forecasting system for seasons that couples the sea, land and air and our atmospheric model is a global forecasting system from NCEP[9] with the initial atmospheric condition extracted from the second set of NCEP reanalysis. For the oceanic module, it is the Model V3.0 from the Geophysical Fluid Dynamics Laboratory of National Oceanic and Atmospheric Administration, USA, with the initial conditions taken from the data of Global Ocean Data Assimilation. In the horizontal direction, the model takes a 62-wave triangle truncated spectrum and is vertically divided into 64 sigma-layers with the top layer at 0.2 hPa. While the meridional distribution is global, its zonal domain is confined at 74°S–64°N. All together, the CFS possesses 28 years of historical forecasts covering 1981–2008 as well as real-time forecasting output (which includes forecasts for nine months ahead). For details, see Saha et al.[11]. Developing a statistical downscaling method based on the output of CFS, this work aims at providing fresh ideas and methods for the prediction of seasonal precipitation in Guangdong.

2 DATA AND METHODOLOGY

The data used in this work include those of precipitation from 86 meteorological stations in Guangdong in 1961–2009, monthly mean reanalysis of NCEP, including geopotential heights, wind fields and relative humidity, and forecasts from CFS.

The methods used include the EOF analysis, OSR[12] and multivariate mean generating function (hereafter MMGF)[13].

3 VERIFICATION OF MODEL PERFORMANCE

To demonstrate the good capability of CFS in simulating the changes in seasonal circulation, we compared the differences between the wind, geopotential height, temperature and sea surface temperature (SST) fields of June–August and that of NCEP. Fig. 1 gives differences in 850-hPa and 200-hPa wind fields between the CFS forecasts and NCEP observational data. Fig. 1 shows that the CFS is capable of simulating features like lower-level cross-equatorial flow, Southwest Monsoon, upper-level monsoonal easterly and South Asia High in summer (figure omitted), but as compared to the observational data (Fig. 1a) its simulations of the lower-level southeast trade wind over the Indian Ocean, Somali Jet and subtropical high in the western Pacific are relatively weak (Fig. 1c), and those of upper-level monsoonal easterly and South Asia High are also relatively weak (Fig. 1d). The CFS also gives similar results for the geopotential heights at 500 hPa (figure omitted).

For the surface temperature field, the CFS simulations differ from the observational data mainly in the cold error over the Asian continent (Fig. 2b). Yang et al.[14] conducted vertical integration of the temperature for the three layers of 850, 500 and 200 hPa and computed its meridional gradient (Fig. 3). As

shown in the result, the meridional gradient of tropical temperature determined with the observational data starts to be positive, or, warmer in the north than in the south, from spring onwards, reaching the maximum in July in the area west of 90°E between 10° and 30°N (Fig. 3a and Fig. 3c). For the meridional and temporal distribution, likewise, the results of the CFS simulation are smaller than those of the observational data (Fig. 3b and Fig. 3d), except for the area in 20–25°N in April and May. It then shows that the CFS simulations reflect a correlation between weak large-scale monsoonal circulation and weak meridional temperature gradient. It is also why the CFS simulations are relatively weak as compared to the NCEP observational data. In spite of what is presented above, the CFS is, generally speaking, able to simulate the variations of large-scale circulation in June–August.

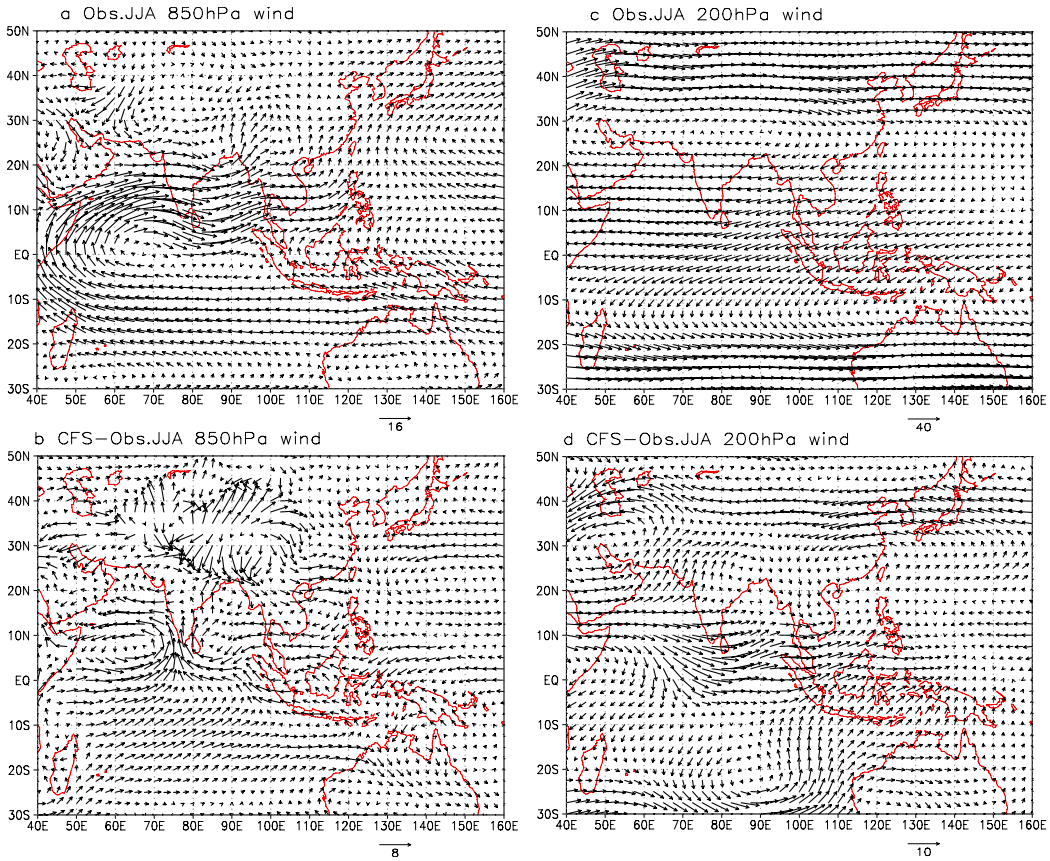

Figure 1. Climatological mean of the wind field for June to August from 1981 to 2008 for the NCEP data at 850 hPa (a), differences between CFS and NCEP (b), NCEP data at 200 hPa (c) and differences between CFS and NCEP (d).

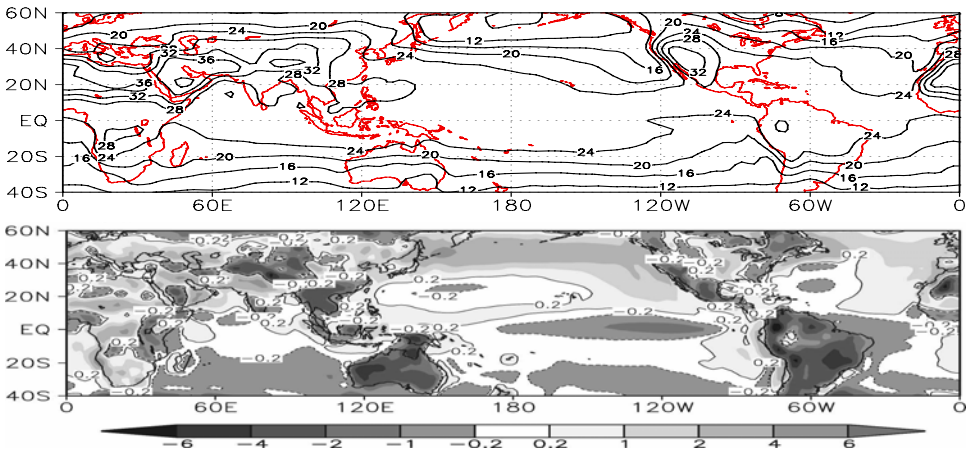

Figure 2. Climatological mean of the surface temperature field at 850 hPa for June–August from 1981 to 2008. (a): NCEP data; (b): differences between CFS and NCEP.

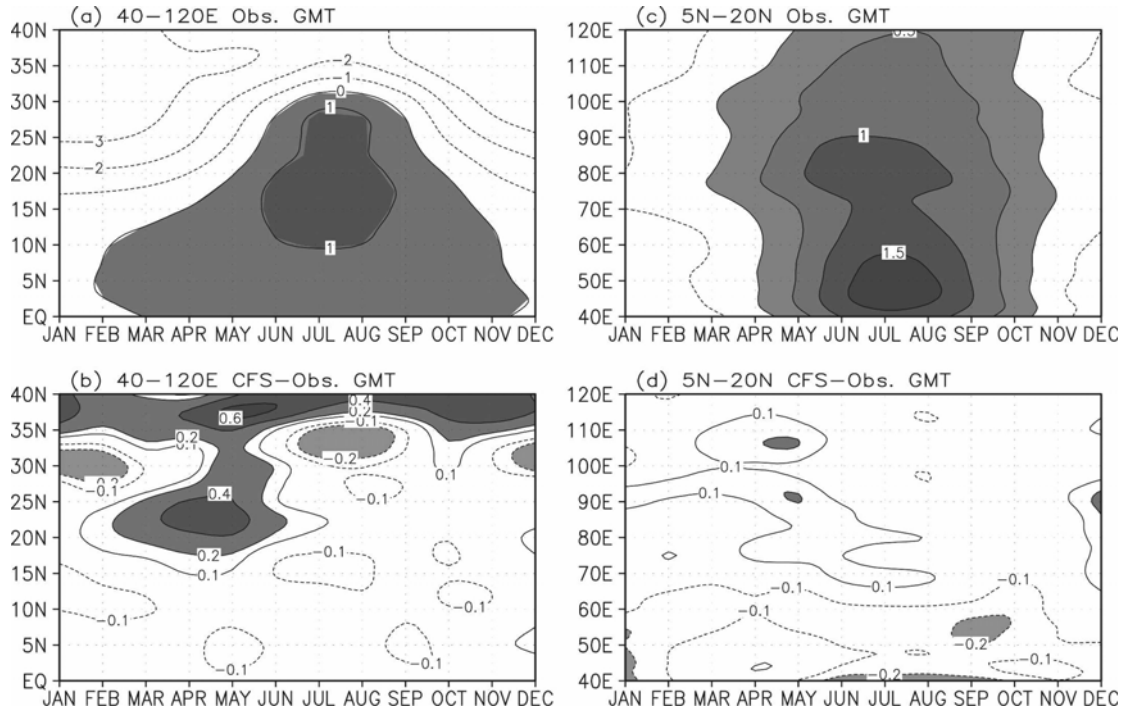

Figure 3. Latitude-time distribution of the NCEP observations (a) and the CFS simulations (b) averaged over 40−120°E and longitude-time distribution[14] of the NCEP observations (c) and the CFS simulations (d) averaged over 50−20°N.

In addition, the CFS is also good at simulating the distribution of anomalous SST and the meridional expansion of warm SST[14]. Despite that the simulations overestimate the actual SST anomalies (SSTA) in the equatorial central Pacific, the CFS is still able of predicting the anomalous evolvement of Pacific SST four months ahead and that of Indian Ocean SST two months in advance. Besides, the CFS is also good at simulating the SSTA within such a small region as the South China Sea and predicting the SSTA of the Pacific during the decaying phase of ENSO five months in advance. Like the developing year of ENSO, however, the CFS-forecast SSTA of the tropical central and eastern Pacific are higher than that of the observation.

In summary, the CFS is capable of simulating the seasonal change in monsoonal circulation in June−August, the evolution of SSTA during the developing and decaying stages of ENSO several months ahead and the variation of circulation in other seasons (figure omitted). For this reason, it is used as a way of research in this study.

4 SELECTION OF THE PREDICTORS

As already shown in some studies[15-25], the western subtropical high, Aleutian low, monsoons and Southern Hemisphere circulation are the systems that can affect the precipitation of the annually first raining season (from April to June) in South China. Their main elements are the 500-hPa geopotential heights, zonal wind, meridional wind and sea level pressure. On the basis of preceding research, the subsets of predictors used in this work for predicting the seasonal precipitation in Guangdong are the gridpoint data of mean sea level pressure, *u* and *v* wind fields, and geopotential height fields at 200, 500 and 850 hPa. In view of the huge amount of data involved with each of the subsets that could lead to lengthy computation, the current study relies on the method of simultaneous correlation to determine the predictors for the four seasons and the annual two seasons of rain in the steps presented as follows. Correlation is sought between the time series of precipitation anomalies and meteorological elements averaged over different seasons for the 86 stations in Guangdong province and the SST field and a significance test is performed on the result. If the region passing the significance test is as large as or more than 100 square degrees of longitude by latitude and what the same-sign anomaly covers is as large as or more than 1,000 square degrees of longitude by latitude, the meteorological elements therein will be averaged by area to obtain the series of predictors. For a single element and a single period of time, if there is more than one region of significance, then one with the largest area of significance will be selected. As a result, primary factors for this study include the sea level height field, wind field (at 200 and 850 hPa) and geopotential height field (at 200, 500 and 850 hPa), which are presented in detail in Tables 1–6.

Table 1. Predictors for winter.

Short forms of the predictors	Areas to choose predictors from	Correl.

mslp	0 °~180 °~0 °, 60 °S~30 °N	+
	70 °E~180 °, 20 °S~20 °N	+
	160~70 °W, 35 °S~10 °N	–
	160~40 °W, 20 °S~40 °N	–
uwnd200	0~150 °E, 25 °Sv25 °N	+
	150 °E~60 °W, 5~25 °N	+
	40 °W~0 °, 15 °S~15 °N	+
	130 °E~120 °W, 70~55 °S	–
	60 °W~0 °, 70~55 °S	–
uwnd850	10~160 °E, 10~30 °N	+
	170 °E~120 °W, 15 °S~10 °N	+
	60~150 °E, 40~20 °S	+
	160 °E~40 °W, 5~20°N	+
	0 °~60 °W, 65~55 °S	–
vwnd200	140 °E~160 °W, 0~25 °N	+
	160 °E~130 °W, 30~10 °S	–
vwnd850	160 °E~120 °W, 40~10 °S	+
	130 °E~120 °W, 5 °S~20 °N	–
Hgt200	0 °~180 °~0 °, 90~60 °S	+
	30~130 °E, 25~35 °N	–
Hgt500	0 °~180 °~0 °, 90~65 °S	+
	70~170 °E, 10 °S~10 °N	+
	160v80 °W, 20~35 °N	–
	160 °E~130 °W, 65~40 °S	–
Hgt850	0 °~180 °~0 °, 90~60 °S	+
	80 °E~180 °, 25 °S~10 °N	+
	170~80 °W, 30 °S~35 °N	–

Table 2. Predictors for spring.

Short forms of the predictors	Areas to choose predictors from	Correl.
mslp	30~110 °E, 10 °S~30 °N	+
	135 °E~170 °W, 20 °S~15 °N	+
	180 °~120 °W, 30~60°N	–
	70~30 °W, 10~20 °N	–
uwnd200	0~80 °E, 20 °S~15 °N	+
	160 °E~110 °W, 80~65 °S	–
uwnd850	180 °~40 °W, 30 °S~10 °N	+
	120 °E~120 °W, 10~30 °N	+
	170~50 °W, 70~50 °S	+
	180 °~110 °W, 40~70 °N	–
vwnd200	170 °E~130 °W, 5 °S~10 °N	+
	90 °E~160 °W, 90~80 °S	–
vwnd850	80~40 °W, 90~55 °S	+
	170~100 °W, 90~40 °S	–
	170 °E~120 °W, 5 °S~10 °N	–
Hgt200	140 °E~130 °W, 40~60 °N	–
	110~60 °W, 80 °S~55 °N	+
Hgt500	130~70 °W, 90~55 °S	+
	180 °~100 °W, 35~55 °N	–
Hgt850	30~100 °E, 10 °S~25 °N	+
	140 °E~170 °W, 25 °S~15 °N	+
	180 °~120 °W, 30~55 °N	–
	100~50 °W, 25~35 °N	–

Table 3. Predictors for summer.

Short forms of the predictors	Areas to choose predictors from	Correl.
mslp	70~150 °E, 30~40 °N	–
uwnd200	170~60 °W, 45 °S~30 °N	+
	170~20 °W, 65~70 °S	–
uwnd850	150~30 °W, 40~30 °S	+
	120~20 °W, 65~55 °S	–
Hgt200	180 °~110 °W, 50~30°S	–
Hgt500	170~120 °W, 55~30 °S	–
Hgt850	180 °~40 °E, 25 °S~10 °N	–

Table 4. Predictors for autumn.

Short forms of the predictors	Areas to choose predictors from	Correl.
mslp	120 °E~180 °, 60~80 °N	+
	60~0 °W, 60~30 °S	–
uwnd200	50~0 °W, 55~35 °S	+
	60~0 °W, 25~35 °N	+
	130~100 °W, 80~90 °N	–
	30~90 °E, 60~75 °N	–
uwnd850	70~170 °E, 80~90 °N	+
	70~0 °W, 50~30 °S	+
	60 °E~180 °, 45~75 °N	–
vwnd200	160 °E~160 °W, 70~90 °N	+
vwnd850	80 °W~0 °, 75~90 °N	+
	160 °E~120 °W, 70~90 °N	–
Hgt200	0~170 °E, 75~90 °N	+
Hgt500	80~170 °E, 70~90 °N	+
Hgt850	100 °E~180 °, 65~80 °N	+
	60 °W~0 °, 65~35 °S	+

Table 5. Predictors for April-June.

Short forms of the predictors	Areas to choose predictors from	Correl.
mslp	170~115 °W, 35~55 °N	–
uwnd200	160 °E~120 °W, 25~30 °N	+
	170~100 °W, 45~60 °N	–
uwnd850	120 °E~120 °W, 10~30 °N	+
	120 °E~60 °W, 35~60 °N	–
Hgt200	120 °E~120 °W, 28~40 °N	–
Hgt500	130 °E~120 °W, 30~40 °N	–
Hgt850	120 °E~120 °W, 30~40 °N	–

Table 6. Predictors for July-September.

Short forms of the predictors	Areas to choose predictors from	Correl.
mslp	20~55 °E, 35~10 °S	+
	170~130 °W, 10 °S~10 °N	–
uwnd200	180 °~0 °, 45~35 °S	+
	60~20 °W, 65~55 °S	+
uwnd850	130 °E~180 °, 5 °S~15 °N	+
	120~90 °W, 5 °S~20 °N	+
vwnd200	130~100 °W, 25 °S~0 °	+
Hgt850	180 °~80 °W, 25 °S~5 °N	–

5 RETROSPECTIVE FORECASTS AND

VERIFICATION

First, the empirical orthogonal function (EOF) is used to decompose the precipitation from the 86 stations by season to determine the main modes (which take up 70% of the total variance) that have been verified. Then, with the methods of OSR and MMGF the time series of the main modes are screened for optimal predictors. At last, the time series so obtained are regrouped with the spatial field to construct the forecast results for the precipitation field of different seasons.

To verify whether the forecast outcomes are feasible, an assessment approach, which was formulated by a department on disasters prediction and mitigation at China Meteorological Administration, is used in the verification. The method is constituted on the basis of the percentage of accurate forecasts of anomaly signs in addition to weighting that varies with the level of anomalies. With the method, the total score for the domain of forecast is thus expressed as:

$$\mathrm{PS} = \frac{N_0 + P_1 N_1 + P_2 N_2}{N + P_1 N_1 + P_2 N_2} \times 100\%$$

where PS is the score for prediction, N the sum of the meteorological stations included in the score statistics, N_0 the sum of the stations for which the anomaly sign of the prediction is the same as that of the observation and those for which the anomaly sign of the prediction is different from that of the observation but the anomaly is only one level apart from each other, N_1 the number of stations for which both the prediction and observation have anomalously more or less precipitation, and N_2 the number of stations for which both the prediction and observation have exceptionally more or less precipitation. P_1 is the weighting coefficient used in adding scores when predicting successfully the anomalously more or less precipitation and P_2 the weighting coefficient used in adding scores when predicting successfully the exceptionally more or less precipitation. Table 7 gives individual ranges of precipitation in tendency scoring.

Table 7. Classification of rain tendency in the scoring system

Terms used in rain prediction	Percentage of anomalies(△ R)/%
Exceptionally less	△ R≤ −50
Anomalously less	−50<△ R≤ −20
Slightly less	−20<△ R<0
Slightly more	0≤ △ R<20
anomalously more	20≤ △ R<50
Exceptionally more	△ R≥ 50

In view of the lack of ways to verify seasonal prediction of precipitation, this study verifies the result by month, the usual way of verification. Retrospective scores (Tables 8–12) are determined for every season in 2001–2008 following the expression above.

It is shown in the PS scores for short-term climate prediction that the average score is above 60 points for most of the seasonal precipitation during this period of time in Guangdong using the OSR with CFS outputs (Table 8). In contrast, the method of OSR is slightly better than that of MMGF when it comes to the forecast of summer, autumn and winter precipitation in Guangdong. For the multi-year mean of retrospective forecasts of the winter and autumn precipitation, the latter method gives the result of 44.61 and 57.84 respectively (Table 9).

Table 8. PS scores of retrospective prediction using the OSR with CFS.

year	1st raining season	2nd raining season	spring	summer	autumn	winter
2001	59.98	76.22	68.79	98.87	47.37	48.86
2002	96.51	82.44	69.23	58.14	77.05	86.11
2003	60.47	73.77	92.27	96.51	65.26	93.43
2004	94.19	92.63	57.17	98.84	22.79	12.16
2005	88.0	60.47	51.14	61.63	81.72	99.31
2006	87.43	62.84	78.11	90.87	69.77	97.96
2007	83.82	91.26	79.31	70.00	95.08	12.64
2008	28.67	71.11	74.01	15.61	60.22	45.25
Mean	74.88	76.34	64.12	73.81	64.91	61.97

Table 9. PS scores of retrospective prediction using the MMGF with CFS.

year	1st raining season	2nd raining season	spring	summer	autumn	winter
2001	67.44	98.24	83.72	98.34	66.48	88.37
2002	56.98	58.62	53.49	58.14	11.63	39.53
2003	73.26	24.57	94.90	66.28	74.85	23.79
2004	96.55	83.15	24.86	44.19	98.42	28.99
2005	54.65	91.86	72.09	94.19	74.16	99.30
2006	45.35	94.19	50.00	66.28	72.09	97.97
2007	76.44	90.86	63.22	93.02	27.91	13.14
2008	70.93	70.93	92.71	65.91	37.14	64.02
mean	67.70	76.56	66.88	73.29	57.84	44.61

Table 10. PS scores of retrospective prediction using the OSR with NCEP

year	1st raining season	spring	autumn	winter	Jun.	Jul.	Aug.	Sept.
2001	84.88	91.86	36.66	84.88	57.06	97.00	71.91	68.36
2002	77.67	81.86	37.44	77.91	93.02	90.53	92.82	22.03
2003	73.26	79.07	55.81	98.83	79.27	99.23	58.29	26.57
2004	79.35	60.47	87.21	96.81	67.57	59.3	38.98	89.64
2005	82.56	66.28	30.99	98.83	60.00	97.13	59.05	41.38
2006	68.97	60.47	77.91	92.59	75.28	91.87	49.13	85.54
2007	80.68	97.82	36.72	54.95	39.53	20.00	82.70	76.72
2008	75.58	97.67	32.57	19.20	41.86	50.00	55.81	46.89
mean	77.87	79.43	49.41	78.00	64.20	75.64	63.59	57.14

Table 11. PS scores of retrospective prediction using the MMGF with NCEP.

year	1st raining season	spring	autumn	winter	Jun.	Jul.	Aug.	Sept.
2001	97.00	82.56	58.19	84.88	84.95	98.97	61.85	83.25
2002	23.95	87.21	29.30	77.91	55.43	94.19	70.81	47.12
2003	93.02	98.84	72.83	45.35	58.14	25.58	49.45	39.89
2004	39.53	96.51	43.02	97.67	32.56	57.78	68.97	81.82
2005	33.72	81.61	22.99	38.67	96.51	76.34	80.81	81.92
2006	98.84	55.81	75.87	83.80	68.72	23.87	56.32	21.14
2007	81.40	79.43	59.16	58.70	41.86	14.65	27.68	48.28
2008	96.80	88.37	39.88	19.20	78.16	67.05	65.03	45.98
mean	66.32	83.79	50.16	63.27	64.54	57.30	60.12	56.18

Table 12. PS scores of rainfall prediction for different periods of time in 2009/2010.

Periods of time	Optimal subsets		Multivariate mean generation function	
	NCEP	CFS	NCEP	CFS
Winter (Dec.—subsequent Feb.)	92.5	93.2	10.3	91.9
Spring (Mar.—May)	89.5	35.6	62.8	62.8
1st raining season (Apr.—Jun.)	72.3	75.3	66.7	68.6
Summer (Jun.—Aug.)	—	68.9	—	82.5
2nd raining season (Jul.—Sept.)	—	56.4	—	62.2

The CFS forecast of winter precipitation varies much in a year with the best being 99.31 and the worst only 12.64. What is behind the striking difference? Is it that the CFS is intrinsically unstable in the seasonal forecast? Here in this section, the years 2004 and 2005 will be studied for their respective highest and lowest PS scores. The factors selected in the two models for retrospective forecasting are different (due to different thresholds of selection), which include the wind fields for 200 and 850 hPa as well as the geopotential height at 500 hPa. From the viewpoint of multi-year mean, or either in terms of the climatological state or the 850 or 200 hPa wind field, the CFS is able to simulate the wintertime circulation well (figure omitted), but it yields weaker-than-observation East Asian Trough, North American Trough, Australian High, equatorial trade wind zone and upper-level westerly, due to systematic errors. Similar situations are also shown in the comparisons of the CFS simulations of the 2004 and 2005 wind fields (figure omitted). The 850-hPa wind in retrospective forecasting for the two years are very close to that of NCEP as far as the tendency is concerned (Fig. 4 and 5). In 2004, the Aleutian low and equatorial trade wind had anomalous enhancement while the Australian high had anomalous reduction, and in 2005, the Aleutian low and the Australian high had anomalous enhancement while the equatorial trade wind had anomalous reduction. They are all well simulated by the CFS. Similarly, simulations are also good of the 200-hPa wind field (figure omitted), like the anomalous enhancement of upper-level westerly. Besides, the CFS is consistent with the NCEP in forecasting the climatological state (figure omitted) and the wintertime circulation for 2004 (Fig. 6c) and 2005 (Fig. 7c) but yields weaker East Asian Trough, North American Trough and Australian High due to systematic errors, with good tendency forecast though (Fig. 6d and 7d). Some other cases (like the highest-scored 2006 and second lowest-scored 2007) are also compared and similar results are obtained. It can then be concluded that the CFS is quite stable on the seasonal scale because it can simulate the anomalies of the circulation field. The discrepancies presented above may be caused by the differences in the factors selected from year to year, which result in different weighting coefficients. More work needs to

be done in the future to optimize the factors to increase the forecasting accuracy.

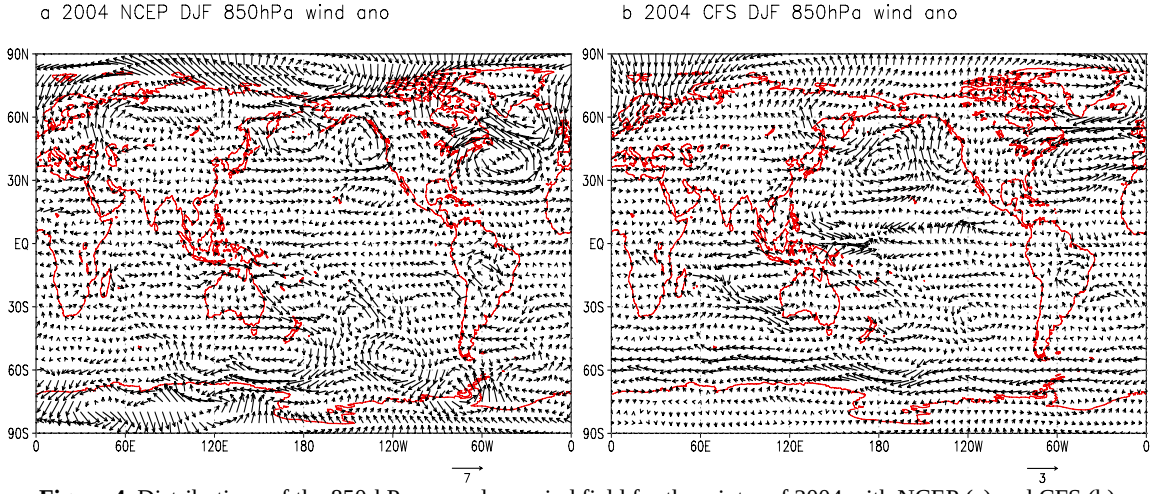

Figure 4. Distributions of the 850-hPa anomalous wind field for the winter of 2004 with NCEP (a) and CFS (b).

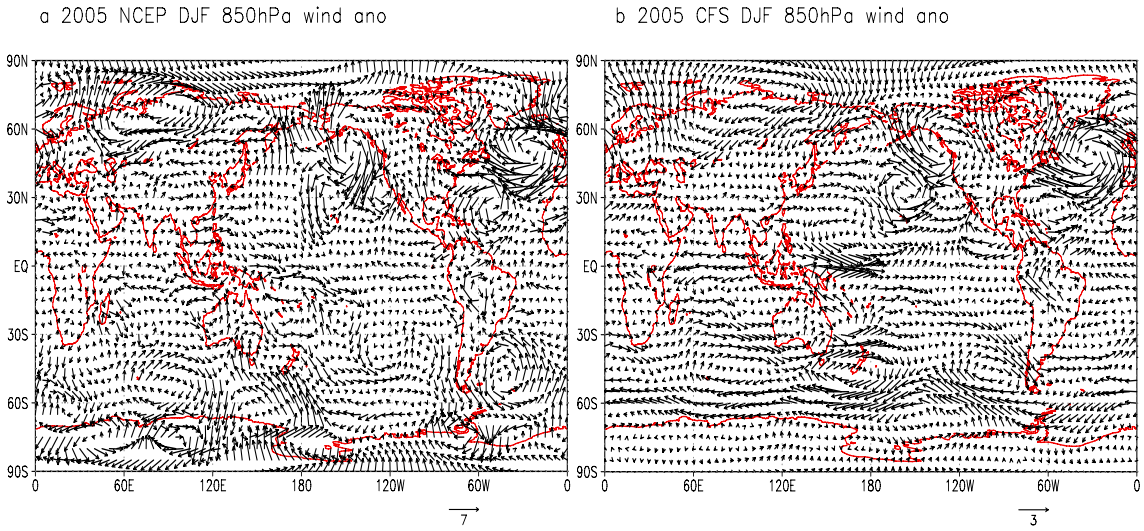

Figure 5. Same as Figure 4 but for 2005.

In addition, the time series used in the CFS for mode construction and fitting is for 1981 to 2000 (20 years). Its length can be as long as 27 years when 2008 is the year to be forecast. Generally speaking, the mean PS score is above 60 points for most of the seasonal prediction of the precipitation in Guangdong, suggesting that it is feasible to use the data in forecasting.

To further demonstrate the feasibility of using CFS outputs in establishing a downscale predictive model for the precipitation of Guangdong, a traditional statistics model (derived by studying preceding predictors based on observations) is used. The NCEP data is screened for factors that are significantly related with precipitation from the temperature fields at 200, 500 and 850 hPa, the geopotential height fields at 200 and 500 hPa, and the wind fields at 200 and 850 hPa. The selection follows the procedure for the CFS outputs. Then retrospective forecasting is conducted to determine various scores for predicting climatological precipitation for different seasons in Guangdong (Tables 10 and 11). It is clear that the precipitation predicted with the OSR with the NCEP data is better than that of the CFS for the annually first raining season, spring and winter, especially the latter two seasons. Their scores for precipitation in Guangdong are 79.43 and 64.12 points for spring and 78 and 61.97 points for winter, respectively. As no predictors from the NCEP data are included in the section for the precipitation in summer and the annually second raining season, predictors are sought individually for June, July, August and September. As shown in the results, the score for July is the best while that of September the worst, the mean PS score for June to August is not as good as that with the CFS and the average for July to September (the annually second raining season) is also not as high as that of the CFS. As compared to the three methods, the MMGF with the NCEP data is generally the worst in the prediction of precipitation

in Guangdong, with the exception of the spring and summer when it is better than that with CFS. It is then clear that the seasonal prediction models set up with the conventional statistics method and the CFS outputs are each advantageous on their own and both produce consistent forecasts of precipitation on the seasonal scale, suggesting that the CFS output works in predicting the precipitation of Guangdong.

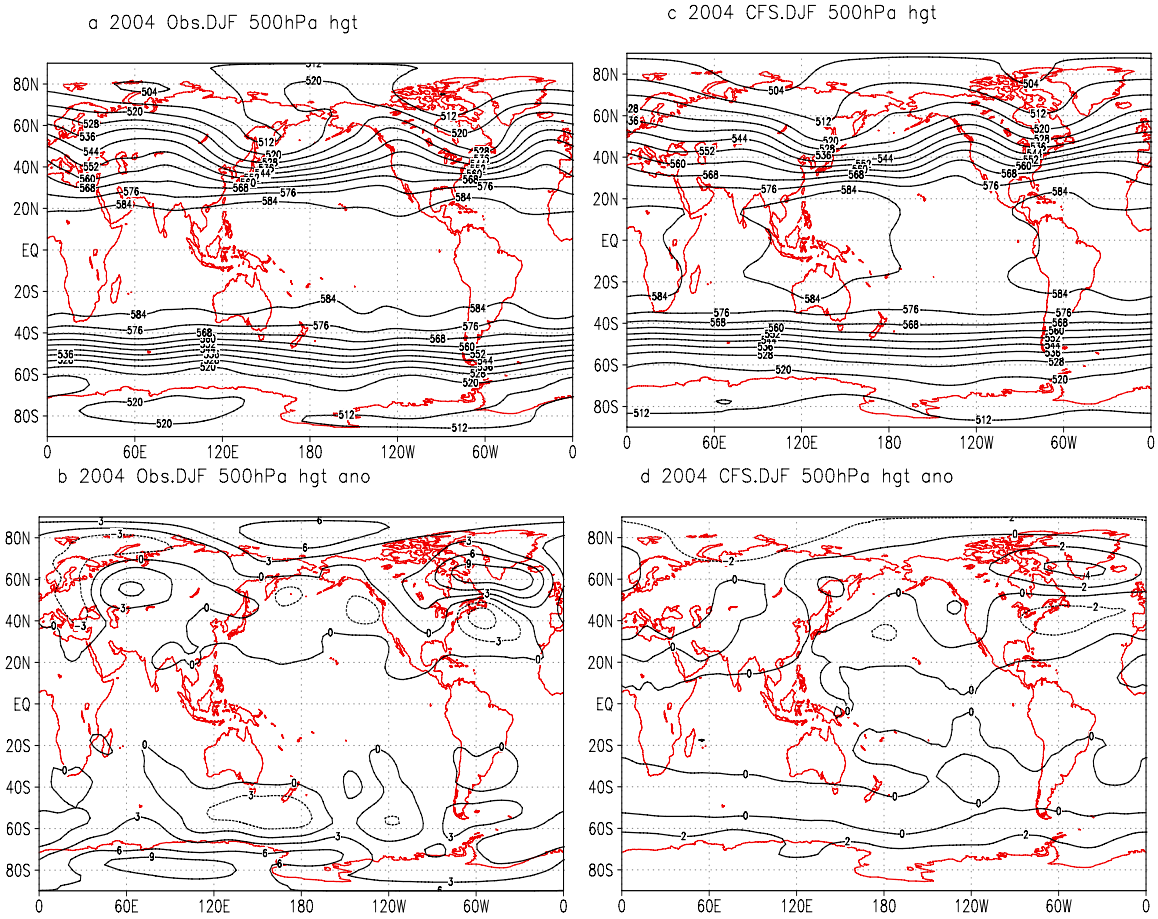

Figure 6. The original fields (a, c) and anomalous fields (b, d) of the 500-hPa geopotential field for the winter of 2004 with NCEP (a, b) and CFS (c, d).

Table 12 presents the PS scores with the four methods in predicting models in making real-time seasonal precipitation forecasts for 2010. It shows that the winter result is the best in which three models (the CFS and NCEP with the OSR as well as the CFS with the MMGF) scored at more than 80 points, followed by the spring result in which one model (the NCEP with the OSR) scores over 80 points, and the raining season (the annually first one) result in which two models (the CFS and NCEP with the OSR) score over 70 points, and the summer result in which one model (the CFS with the MMGF) scores more than 80 points. The result for the annually second raining season is the worst of all. Intercomparisons between individual models indicate that the NCEP with the OSR is the most stable model that yields scores of 92.5, 89.5 and 72.3 points for the forecasts of the winter, spring and the annually first raining season, respectively. The CFS with the OSR scores the highest (93.2 points) for winter prediction and second highest (72.3 points) for the annually first raining season. The NCEP with the MMGF performs the worst with none of the predictions achieving 70 points. The CFS with the MMGF scores higher for the winter and summer prediction, 91.9 and 82.5 points, respectively. In summary, the NCEP with the OSR has the best performance while the NCEP with the MMGF performs worst, with the other two models varying in stability.

It is known from the analysis above that the results from the CFS output is generally close to that achieved with the conventional observations, scoring more than 60 points on average though with large intra-annual fluctuations in some seasons. Besides, the CFS products are updated in real time, being capable of forecasting the precipitation of Guangdong three seasons ahead, while the traditional statistical method is not good at forecasting some of the seasons due to the limitation of the NCEP reanalysis in addition to the absence of some predictors in the forecasting models due to updating. It is now known that uncertainty exists in the precipitation forecast with the

statistical method such that one of them cannot be replaced with another all together. The downscaling predictive model of this present work, which is used to forecast the seasonal precipitation of Guangdong, enriches the conventional statistical method but needs further improvement in the stability of forecasts. If these four methods—set up with the CFS outputs and NCEP reanalysis—can be combined for perfection and new downscaling methods can be developed, the forecasting of precipitation can be made better.

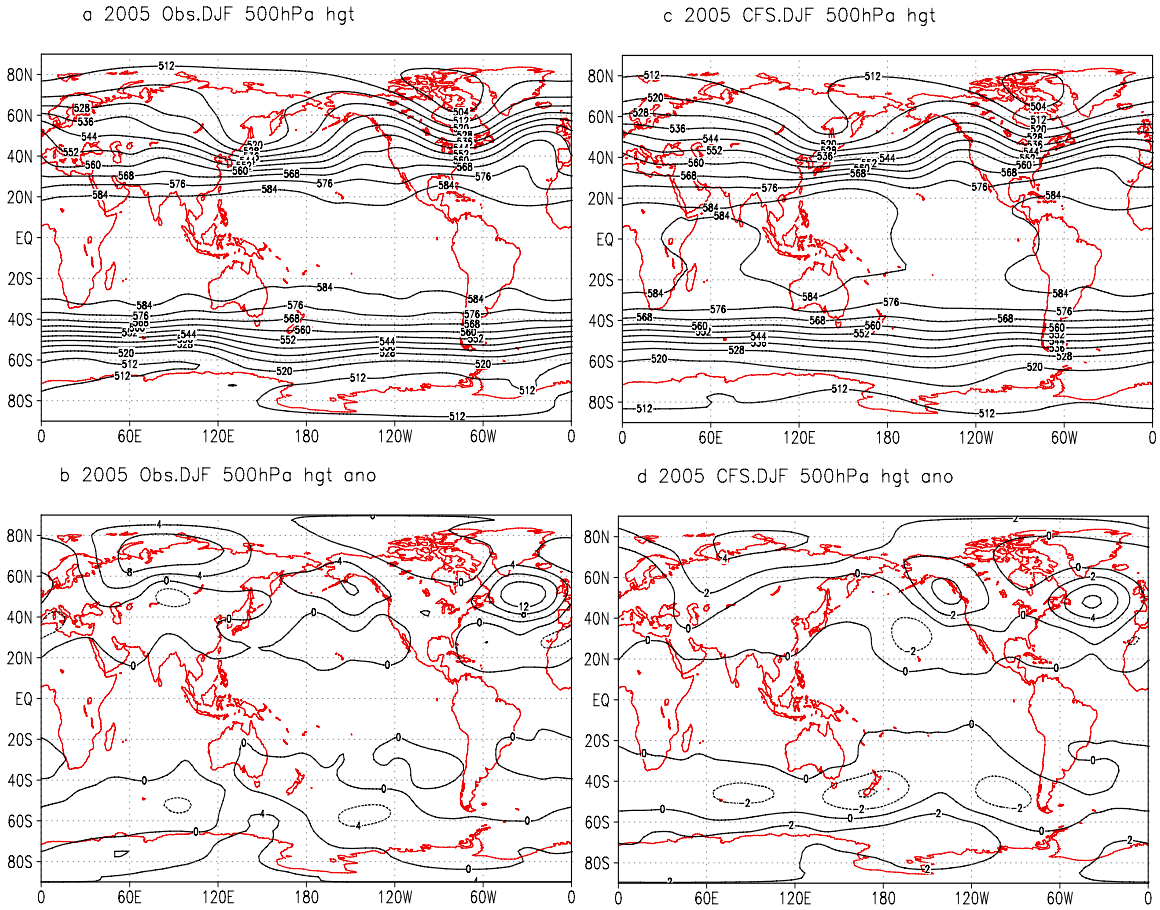

Figure 7. Same as Fig. 6 but for 2005.

6 CONCLUSIONS

The retrospective forecasting data of the CFS spans from 1981 to 2008 (28 years), which include both real-time and 9-month forecasts. Compared to the NCEP data, the CFS is able to simulate the seasonal variation of monsoon circulation, especially the anomalous development of sea surface temperature during the evolution and decay stage of ENSO, with a lead of a few months. Therefore, the CFS data can be used for forecasting precipitation in Guangdong.

In this work, the CFS outputs are used to develop downscaling methods that are based on the OSR and the MMGF. Following our analysis and verification, mean sea level pressure, wind and geopotential height are selected as the concurrent predictors. Retrospective forecasting and verification for multiple years have shown that the CFS outputs with the OSR perform a little better than that with the MMGF in the forecast of the precipitation in the annually first raining season, summer, autumn and winter, especially the winter and autumn. The NCEP with the OSR is superior over the CFS in the forecast of precipitation in the annually first raining season, spring and winter. The retrospective forecast of seasonal precipitation with the CFS outputs is marked with intra-annual instability for some seasons. As shown in the analysis, it is independent of the instable performance of the CFS outputs but may be related to the difference in the predictors selected for each of the years of interest such that the weighting coefficient varies. More work is needed in this aspect. Besides, in the PS scores for real-time prediction of seasonal precipitation in 2009 and 2010, the NCEP with the OSR gives the best prediction while the NCEP with the MMGF yields the worst, with the other two models varying in stability.

In general, as compared with the conventional way of statistical approach with the NCEP data, the

CFS outputs, due to real-time production and rapid updates, are superior such that the downscaling method based on them are able of forecasting the precipitation in Guangdong by a lead of three seasons. It enriches the way of conventional statistical forecasting but needs to be improved in the stability of forecasting.

REFERENCES:

[1] Von S H. Inconsistencies at the interface of climate impact studies and global climate research [J]. Meteorologische Zeitschrift, 1995, 4: 72 280.
[2] Von S H. The global and regional climate system [C]//Anthropogenic Climate Change. Berlin: Springer Verlag, 1999: 3-36.
[3] LU Xin-ping, CHEN Xing, MIAO Man-qian. The study of initial data preprocessing in the downscaling method [J]. Sci. Meteor. Sinica, 2002, 22(2): 139-148.
[4] CHEN Li-juan, LI Wei-jing, ZHANG Pei-qun. Application of a new downscaling model to monthly precipitation forecast [J]. Quart. J. Appl. Meteor., 2003, 14(6): 648-655.
[5] FAN Li-jun, FU Cong-bin, CHEN De-liang. Estimation of local temperature change scenarios in North China using statistical downscaling method [J]. Chin. J. Atmos. Sci., 2007, 31(5): 887-897.
[6] DING Yu-guo, LIU Ji-feng, ZHANG Yao-cun. Simulation tests of temporal-spatial distributions of extreme temperatures over China based on probability weighted moments estimation [J]. Chin. J. Atmos. Sci., 2002, 28(5): 771-782.
[7] HE Hui, JIN Long, QIN Zhi-nian, et al. Downscaling forecast for the monthly precipitation over Guangxi based on the BP neural network model [J]. J. Trop. Meteor., 2007, 23(1): 72-77
[8] WEI Feng-ying, HUANG Jia-you. A study of predictability for summer precipitation on East China using downscaling techniques [J]. J. Trop. Meteor., 2010, 26(4): 483-488.
[9] MOORTHI S, PAN H L, CAPLAN P. Changes to the 2001 NCEP operational MRF/AVN global analysis/forecast system [R]. NWS Tech. Procedures Bull., 2001: 484, 14.
[10] PACANOWSKI R C, GRIFFIES S M. MOM3.0 manual [R]. NOAA/GFDL, Princeton, NJ, 1998: 8542.
[11] SAHA S, NADIGA S, THIAW C, et al. The NCEP climate forecast system [J]. J. Climate, 2006, 19(15): 3483-3517.
[12] WEI Feng-ying. Techniques of Statistical Diagnostics and Prediction for Modern-Times Climate [M]. Beijing: China Meteorological Press, 1999: 194-201.
[13] LIN Ai-lan. The multiple mean generational function model and its application in short-range climatic forecast [J]. J. Trop. Meteor., 2001, 17(3): 287-292
[14] YANG S, ZHANG Z Q, KOUSKY V E, et al. Simulations and Seasonal prediction of the Asian Summer Monsoon in the NCEP climate forecast system [J]. J Climate, 2008, 21: 3755-3775.
[15] LIANG Jian-yin. The interannual variations of the subtropical high ridge position over western Pacific in June and its influence on precipitation in south of China [J]. J. Trop. Meteor., 1994, 10(3): 274-279.
[16] QIN Wu, SUN Zhao-bo, DING Bao-shan, et al. Precipitation and circulation features during late-spring to early-summer flood rain in south China [J]. J. Nanjing Inst. Meteor., 1994, 17(4): 455-461.
[17] DENG Li-ping, WANG Qian-qian. On the relationship between precipitation anomalies in the first raining season (April-June) in southern China and SST over offshore waters in China [J]. J. Trop. Meteor., 2002, 18(1): 44-55.
[18] GUO Qi-yun, SHA Wan-ying. Analysis of rainfall variability during the first rainy season in South China [J]. Quart. J. Appl. Meteor., 1998, 9(suppl.): 9-15.
[19] GAO Bo, CHEN Qian-jin, REN Dian-dong. Diagnostic analysis on the severe drought/flood for the beginning of flood season in southern part of the south of Yangtze River valley and northern South China [J]. Quart. J. Appl. Meteor., 1999, 10(2): 219-226.
[20] CAI Yue-zhan, XU Jin-jing, WU Bin. Relationships Between Typical Droughts and Floods in the Annually First Raining Season and a Number of Preceding Physical Factors [M]//Research on the Methods of Diagnostic Analysis and Prediction of Severe Droughts and Floods and Chilly Weather. Beijing: China Meteorological Press, 2000: 166-173.
[21] TAO Shi-yan. Abnormal Activities of Summer Monsoon in East Asia and Exceptionally Heavy Floods in South China in 1994 (I. Anomalies of the General Circulation) [C]// Proceedings of Seminar on Exceptionally Heavy Floods in South China in 1994. Beijing: China Meteorological Press, 1995: 1-5.
[22] SUN Ying, DING Yi-hui. Role of summer monsoon in anomalous precipitation patterns during 1997 flooding season [J]. Quart. J. Appl. Meteor. 2002, 13(3): 277-287.
[23] WU Shang-sen. Climatic Background for Exceptionally Heavy Rains in South China in 1994 [M]//Research on Exceptionally Heavy Rains in South China in 1994, Beijing: China Meteorological Press, 1996: 23-30.
[24] LI Yu-lan, DU Chang-xuan, TAO Shi-yan. Abnormal Activities of Summer Monsoon in East Asia and Exceptionally Heavy Floods in South China in 1994 (II. Synoptic Analysis of Exceptionally Heavy rains in Guangdong and Guangxi) [C]//Proceedings of Seminar on Exceptionally Heavy Floods in South China in 1994, Beijing: China Meteorological Press, 1995: 6-13.
[25] ZHANG Ai-hua, WU Heng-qiang, QIN Wu, et al. The preliminary exploration for the influence of general circulation over Southern Hemisphere on precipitation over South China during pre-flood season [J]. Meteor. Mon., 1997, 23(8): 9-15.

Citation: LI Chun-hui, LIN Ai-lan, GU De-jun et al. The downscaling forecasting of seasonal precipitation in Guangdong based on climate forecast systems products. *J. Trop. Meteor.*, 2014, 20(2): 143-153.